AN EVALUATION OF WAVE MODEL PERFORMANCES WITH LINEAR AND NONLINEAR DISSIPATION SOURCE TERMS IN LAKE ERIE

Roop Lalbeharry[1], Arno Behrens[2], Heinz Guenther[2] and Laurie Wilson[1]

1. Meteorological Research Branch, Meteorological Service of Canada, Canada
   Roop.Lalbeharry@ec.gc.ca; Lawrence.Wilson@ec.gc.ca

2. GKSS Research Centre, Institute for Coastal Research, Geesthacht, Germany
   Arno.Behrens@gkss.de; Heinz.Guenther@gkss.de

1. INTRODUCTION

Recently new improved versions of different wave models became available and offer the challenge to apply these models to appropriate areas to assess their performances. Three state-of-the-art third generation ocean wave models are used in an intercomparison study, namely, the new WAM Cycle-4.5 (hereafter referred as WAM4.5), the SWAN Cycle III version 40.31 (hereafter referred as SWAN), both of which use a linear dissipation source term, and the K-model which uses a nonlinear dissipation source term. The three models are applied to Lake Erie during a three week hindcast simulation of lake waves with the main inputs to the models being the same wind field and a constant bathymetry. Lake Erie is an inland enclosed body of water whose depth ranges from 5-60 m and can be considered shallow enough to be used as a candidate for testing these models in shallow water mode. The period of study is 12 November - 4 December 2003 and the lake bathymetry and the locations of the buoys used in the verification of model results are shown in Fig. 1 The three models are forced by 10 m level winds at 3-hourly intervals generated by the Canadian Meteorological Centre (CMC) weather prediction model and are spun up for two days to create model initial states prior to the start of the wave simulation runs. The wind dataset is created by assembling the 00, 03, 06 and 09 forecast hours winds of the 0000 UTC and the 1200 UTC daily runs of the CMC weather prediction model to produce a quasi-hindcast wind dataset for the period of this study. The results obtained by each of these models are compared with observations at primarily three buoy locations. Importance is attached to the comparability of the wave models with respect to the source terms included in the models. The primary objective of this study is to assess the performances of these three models in shallow water mode with depth refraction and without tidal influences and to demonstrate the suitability of using the WAM4.5 in an operational environment to produce wave forecasts on an enclosed body of water such as Lake Erie which is dominated mainly by locally generated wind waves. The three models are briefly described in section 2. Model results and discussions are presented in section 3 followed by summary and conclusions in section 4.

2. STATE-OF-THE-ART WAVE MODELS

2.1 Action Density Equation

The ocean waves are described with the two-dimensional wave action density spectrum $N(\sigma,\theta,\phi,\lambda,t)$ as a function of relative angular frequency σ, wave direction θ, latitude ϕ, longitude λ, and time t. $\sigma = [(gk)\tanh(kd)]^{1/2}$ in which k (= $2\pi/L$, L being the wavelength) is the wave number, g is acceleration due to gravity and d is the water depth. The action density spectrum is defined as the energy density spectrum $F(\sigma,\theta,\phi,\lambda,t)$ divided by σ observed in a frame moving with the ocean current velocity, that is, $N(\sigma,\theta,\phi,\lambda,t) = F(\sigma,\theta,\phi,\lambda,t)/\sigma$. The action density is chosen because it is conserved in the presence of time-dependent water depths and currents whereas the energy density spectrum is not. In general, the conservation equation for N in flux form in spherical coordinates and in frequency-direction space is given in the form:

$$\frac{\partial N}{\partial t} \; + \; (\cos\phi)^{-1}\frac{\partial}{\partial\phi}\,(c_\phi\cos\phi N) \; + \; \frac{\partial}{\partial\lambda}(c_\lambda N)$$
$$+ \; \frac{\partial}{\partial\sigma}(c_\sigma N) \; + \; \frac{\partial}{\partial\theta}(c_\theta N) \; = \; \frac{S}{\sigma} \qquad (1)$$

where

$$S \; = \; S_{phil} + S_{in} + S_{nl4} + S_{ds} + S_{bf} \qquad\qquad (2)$$

In (1) the first term on the left hand side represents the local rate of change of action density in time, the second and third terms the propagation of action density in geographical space (with propagation velocities c_ϕ and c_λ in latitude and longitude space, respectively), the fourth term the shifting of the relative frequency due to variations in depths and currents (with propagation velocity c_σ in σ space) and the fifth term the depth-induced and current-induced refraction (with propagation velocity c_θ in θ space). In wave number-direction space k replaces σ and the velocity c_k in wave number space replaces the velocity c_σ in frequency space. For time-independent depth and current, the absolute frequency is conserved when following a wave group and the action density balance equation reduces to the energy balance equation. For no current and time-independent depth c_k = c_σ = 0 and the equations in both k- and σ-space reduce to the energy balance equation, that is, the 4th term on the left hand side vanishes and the depth refraction term (5th term) depends only on the depth gradient.

The term S = $S(\sigma,\theta,\phi,\lambda,t)$ on the right hand side of (1) is the net source term expressed in terms of energy density. It is the sum of a number of source terms given in (2) representing the effects of wave generation by wind (S_{phil} and S_{in}), quadruplet nonlinear wave-wave interactions (S_{nl4}), dissipation due to whitecapping (S_{ds}) and bottom friction (S_{bf}). The linear wind growth term S_{phil} is due to Cavaleri and Malonette-Rizzoli (1981) but with a filter to eliminate contributions from frequencies lower than the Pierson-Moskowitz frequency (Tolman, 1992), and is hereafter referred as CR81. S_{in} is the exponential wind growth source term based on the formulations of Komen et al. (1984) and Janssen (1989, 1991). S_{nl4} is the quadruplet nonlinear wave-wave interactions which transfers energy from spectral peaks to lower and higher frequencies. The energy is redistributed so that there is no net loss or gain of energy due to nonlinear wave-wave interactions. S_{nl4} dominates the evolution of the spectrum in deep and intermediate waters and is computed with the discrete interaction approximation method of Hasselmann et al. (1985) The bottom friction source term S_{bf} is based on the empirical JONSWAP model of Hasselman et al. (1973). The friction dissipation constant Γ in S_{bf} is tuning parameter and is not necessarily the same in the three models.

2.2 **WAM4.5**

The WAve Model WAM solves the energy balance form of (1) for no currents and fixed water depths on a spherical grid and in frequency-direction space. WAMDI Group (1988) describes the Cycle-3 version of WAM (hereafter referred as WAM3) in which S_{in} and S_{ds} are based on the formulations of Komen et al. (1984). In the WAM Cycle-4 version (hereafter referred as WAM4), S_{in} and S_{ds} are based on the formulations of Janssen (1989, 1991) in which the winds and waves are coupled, that is, there is a feedback of growing waves on the wind profile. The effect of this feedback is to enhance the wave growth of younger wind seas over that of older wind seas for the same wind. The WAM4.5 is an update of the WAM4. It uses the first order upwind explicit propagation scheme which results in the propagation time step being limited by the CFL condition and a fully implicit source term integration. To ensure that the WAM remains numerically stable a limitation on wave growth is imposed. This limiter is based on the formulation of Hersbach and Janssen (1999), hereafter referred as HJ99, and gives the maximum total change of energy density per iteration per spectral wave component. It is expressed as

$$|\Delta F(f,\theta)|_{max} = 3.0 \times 10^{-7}gu_*f^{-4}f_c\Delta t \qquad (3)$$

in which f is frequency, u_* friction velocity, f_c model prognostic cutoff frequency and Δt source term integration time step Here $u_* = max(u_*,gf^*_{PM}/f$) and $f^*_{PM} = 5.6 \times 10^{-3}$ is the dimensionless Pierson-Moskowitz frequency. In terms of action density and σ

$$|\Delta N(\sigma,\theta)|_{max} = (2\pi)^2 \times 3.0 \times 10^{-7} gu_*\sigma_c\Delta t/(\sigma^3k) \quad (4)$$

The source term S_{phil} based on CR81 has now been added to WAM4.5 as it was excluded in earlier versions of the WAM. The WAM4.5 run is referred to as run WM1 in the text. More details of the formulation of the WAM can be found in Komen et al. (1994).

2.3 **SWAN**

The SWAN (Simulation of WAves Nearshore) model solves the action balance equation on a spherical grid and in σ-θ space. Because of the assumptions of time-independent water depths and no currents, the solution of (1) is equivalent to the solution of the energy balance equation as in WAM4.5. The propagation scheme is fully implicit and for the source term integration scheme the fully implicit option is chosen. SWAN has the option of using WAM3 or WAM4 physics for the S_{in} and S_{ds} source terms. The version used in this study is the parallelized version with MPI as an option. The

net source term S in (2) includes S_{phil} and the wave growth limiter used in SWAN is described in Ris (1997), hereafter referred as R97. This limiter is given as

$$|\Delta N(\sigma,\theta)|_{max} = (0.1\alpha_{PM})/(2\sigma k^3 c_g) \tag{4}$$

where $\alpha_{PM} = 0.0081$ is the Phillip's constant. The SWAN implementation of WAM4 is not consistent with the actual implementation of WAM4. The shift growth parameter $z_\alpha = 0.011$ in S_{in} is omitted and the limiter R97 instead of HJ99 is used. The modified S_{in} now includes z_α and a new subroutine is added so that when the WAM4 option is used, the limiter HJ99 is called. The model results so produced are now in better agreement with those of WAM4.5. In the text SJ1 refers to the run based on the SWAN implementation of Janssen's WAM4, SJ2 to that based on Janssen's WAM4 but with the modifications described above and SK1 to that based on Komen's WAM3. Table 1 identifies the runs and the physics associated with them. In these runs Γ in S_{bf} is set to the same value as in WAM4.5 and S_{phil} is given by CR81. More details of SWAN are given in Booij et al. (1999), Ris et al. (1999) and of the version 40.31 used in this study in the SWAN User Manual (2004).

Table 1. SWAN run identification and associated physics

Source term	Run ID		
	SJ1	SJ2	SK1
S_{in}	WAM4[+]	WAM4[++]	WAM3
S_{ds}	WAM4	WAM4	WAM3
Limiter	R97	HJ99	R97
+ SWAN implementation of WAM4			
++ SWAN implementation of the modified WAM4			

2.4 K- MODEL

The K-model is developed in the technical frame of WAM4 (Schneggenburger et al., 2000). It describes the evolution of the action density $N(k,\theta)$ in k-θ instead of σ-θ coordinate system and uses the same numerical propagation and integration schemes as those of WAM4.5. For time-independent depth and no currents $c_k = c_\sigma = 0$ and (1) in k-θ system reduces to the energy balance equation as in the cases of WAM4.5 and SWAN. S_{in} is based on WAM3 in which the Snyder wind input (WAMDI Group, 1988) is modified to include the effect of wind gustiness and S_{ds} is a nonlinear dissipation function. In the K-model S_{nl4} is neglected and S_{phil} is reduced to one-tenth of its original magnitude to reduce the input for short waves in small scale applications. The equations for S_{in} and S_{ds} are given by Schneggenburger et al. (2000) as:

$$S_{in} = \beta\sigma G N(k,\theta) \tag{5}$$

in which the gustiness parameter

$$G = \frac{1}{\sqrt{2\pi}}\frac{\sigma_{u_*}}{c_*}\exp[-\frac{(c_* - u_*)^2}{2\sigma_{u_*}^2}] +$$
$$\frac{1}{2}[\frac{u_*}{c_*} - 1][1 - \Phi(\frac{c_* - u_*}{\sigma_{u_*}})]) \tag{6}$$

where

$$c_* = \sigma/[28 k \cos(\theta - \theta_w)] \tag{7}$$

$$\Phi(x) = \frac{2}{\sqrt{2\pi}}\int_0^x e^{\frac{-t^2}{2}} dt \tag{8}$$

$$\frac{\sigma_{u_*}}{u_*} = 0.4 \tag{9}$$

Here, θ_w is the wind direction, $G = 0$ for $\cos(\theta - \theta_w) < 0$, β = constant, Φ is a probability function and σ_{u_*} is the standard deviation of the assumed normal distribution for the friction velocity. In the input source term u_* is replaced by the 10 m level wind speed u_{10} using the fixed relation $28u_* = 1.2u_{10}$.

The nonlinear dissipation function is given by

$$S_{ds} = -\gamma g k^5[\coth(2kd) +$$
$$\frac{kd}{\sinh^2(kd)}]N^2(k,\theta) \tag{10}$$

with

$$\gamma(N) = \gamma_0 \frac{p_1(p_2\frac{k}{\langle k\rangle})^q + 1}{(p_2\frac{k}{\langle k\rangle})^q + 1} \tag{11}$$

where $\langle k\rangle$ is mean wave number. The K-model applies an additional filter to S_{phil} given by CR81 and adopts the HJ99 limiter. The two sets of source term tunable parameters used in this study and given in Table 2 identify the corresponding K-model runs KM1 and KM2 referred to in the text.

2.5 Model implementation

The three models are configured as given in Table 3. In the case of the WAM4.5 and the SWAN the parallelized versions with MPI are used. The models are run in shallow water mode with depth refraction only. It is assumed that there are no currents and that the water depths are time-independent. Fig. 1 shows the computational domain and the bathymetry for Lake Erie with water depths ranging from 5 m to 60 m and the locations of the buoys used in the verification of the model results.

Table 2. K-model tunable parameters and run identification.

		Run ID	
	Parameter	KM1	KM2
S_{in}	β	0.0009	0.0006
S_{ds}	γ_0	0.09485	0.06775
	p_1	10	4
	p_2	1.6	1.2
	q	6	8
S_{bf}	Γ (m^2s^{-3})	0.038	0.01

Table 3. Model domain and configuration

Domain	Lake Erie: 41.30^oN - 43.00^oN 83.60^oW - 78.60^oW
Coord. System	Spherical
Spatial res.	0.05^o x 0.05^o (approx. 4 x 4 km)
Spectral res.	25 frequencies: $f_1 = 0.05$ Hz $f_{i+1}/f_i = 1.1$ 25 wave numbers: $k_1 = 0.01$ m^{-1} $k_{i+1}/k_i = 1.21$ 24 directions: $\Delta\theta = 15_o$ 1st direction = 7.5^o
Grid size	98 x 35
Land+sea pts.	3430
Sea points	1172
Time steps (s)	WAM4.5: $\Delta t_p = 120$, $\Delta t_s = 720$ K-model : $\Delta t_p = 180$, $\Delta t_s = 720$ SWAN : $\Delta t_p = \Delta t_s = 1200$ Δt_p = propagation time step Δt_s = source term integration time step

3. RESULTS AND DISCUSSIONS

Time series plots of buoy and model one-dimensional (1-d) spectra (m^2Hz^{-1}) at 3-hourly intervals in which the energy densities are contoured in terms of color scales are presented in Fig. 2 at buoy location 45132 and in Fig. 3 at buoy location 45005. Buoy 45132 located in water depth of 22 m shows three main wave height episodes while buoy 45005 located in water depth of 14 m shows two main wave height episodes, the wave episode around 15 UTC 13 November being the most pronounced at both buoys. In the discussion that follows the WAM4.5 run is identified as WM1, the SWAN runs as SJ1, SJ2 and SK1 defined in Table 1 and the K-model runs as KM1 and KM2 defined in Table 2.   SJ1 is the SWAN implementation of WAM4 according to the formulation of Janssen (1991) and SK1 that of WAM3 according to the formulation of Komen et al. (1984). The WM1 spectra reveal mainly the same characteristics as the KM2, SJ2 and SK1 spectra which, in turn, agree reasonably well with the buoy spectra.   The KM2 spectra agree much better with the buoy spectra than the KM1 spectra. The results of using the source term tunable parameters in KM2 are consistent with those of Schneggenburger (1998, 2000) in the K-model set-up for fine grid applications in the North Sea and Sylt-Romo Bight. The results demonstrate that the parameters in the K-model set-up in KM2 can also be applied to the grid resolution used here for Lake Erie in shallow water mode.   Run KM2 was rerun but with bottom friction coefficient T = 0.038 m^2s^{-3}. The differences, not shown here, are minimal, indicating that the contribution of the bottom friction source term is not too significant for the wind sea waves generated in Lake Erie.

In the case of the SWAN, SJ1 produces poorer results than SJ2, which implies that the WAM4 physics as implemented in the SWAN may be in error. The results of SJ2 based on the inclusion of the shift growth parameter $z_\alpha = 0.011$ and the wave growth limiter of HJ99 are in good agreement with those of SK1 based on WAM3 physics of Komen et al. (1984).

The peak wave heights of the wave episode around 15 UTC 13 November lie mainly in the frequency range 0.13 - 0.18 Hz when comparing runs WM1 and KM2. The principal function of the nonlinear wave-wave interaction source term S_{nl4} is to redistribute the high frequency energy to lower and higher frequencies with a resultant shift in the frequency of the peak wave energy. The comparison shows that the impact of S_{nl4} is at least minimal so that the nonlinear S_{ds} in combination with the modified S_{in} of WAM3 in KM2 produces results close to those of WM1 which includes S_{nl4} and a quasi-linear S_{ds}. From the comparison of WM1, KM2 and SJ4 spectra it may be concluded that WAM4.5 can be adapted to run in shallow water mode on an enclosed body of water such as Lake Erie and produce results that are consistent

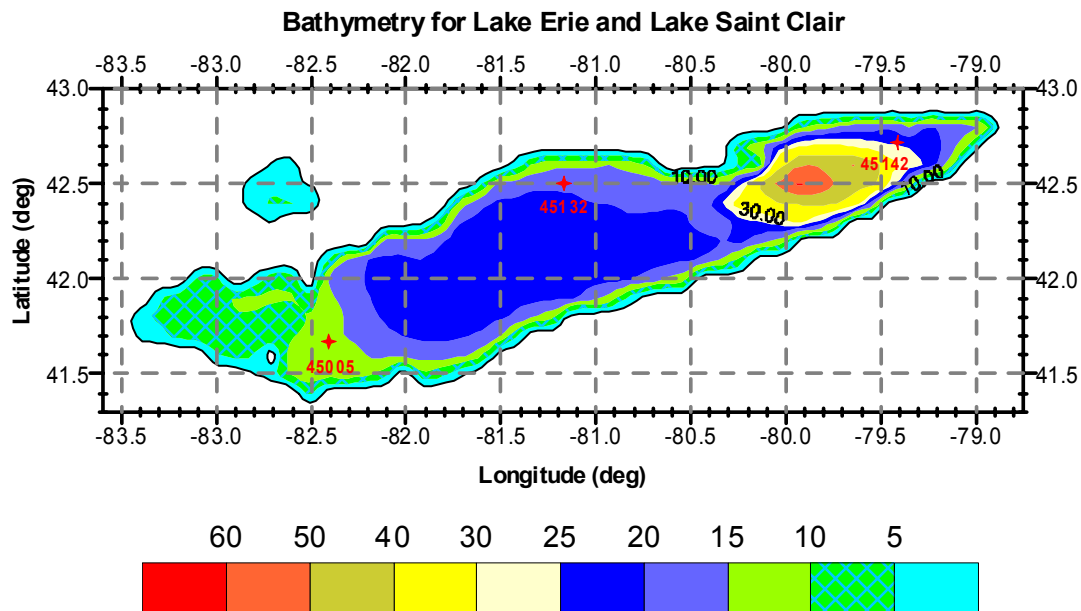## Bathymetry for Lake Erie and Lake Saint Clair

Fig. 1: Lake Erie (and Lake Saint Clair) bathymetry in metres and locations of buoys 45005, 45132 and 45142 used in the verification of model results

with near shore models such as the K-model or the SWAN.

Time series plots of model and observed wave heights and peak periods at buoy 45132 are presented in Fig. 4. Fig. 4a compares run SJ2 (rose curve) and Fig. 4b run SJ1 (rose curve) with runs WM1 (red curve) and KM2 (blue curve) and with the buoy observations (black curve). It can be seen that SJ2 is in better agreement with observations and with WM1 and KM2 than SJ1 for both wave heights and peak periods. This lends some justification to modifying the SWAN implementation of WAM4 as discussed earlier.

Fig. 5 presents scatter plots of model versus buoy wave heights for the period 12 November - 4 December 2003. The plots are based on observations at buoys 45132, 45005 and available observations at buoy 45142 located at the eastern end of the lake. The solid black lines denote perfect fit to model and observed values and the solid red lines the symmetric slope, s, defined in Table 4. The slope, s, is the coefficient of linear regression constrained to pass through the origin. Model values are overpredicted for $s > 1.0$ and underpredicted for $s < 1.0$. The KM1 and SJ1 scatter plots show that model wave heights are grossly underpredicted ($s < 1.0$). The KM2 plot shows that model wave heights in excess of 3.0 m are generated while the KM1 plot shows model wave

heights are all below 3.0 m. The scatter of the KM2 plot is also quite similar to that of the WM1 plot. The SJ2 and SK1 plots are quite similar and show better agreement with observations than the SJ1 plot. In other words, the tunable source parameters for KM2 are more appropriate for the Lake Erie grid resolution used here in producing the higher wave heights. The close agreement between the SJ2 and SK1 suggests that the modified WAM4 option in SWAN, if used, may be expected to produce more accurate wave heights than the SWAN implementation of WAM4. The poorer results of run SJ1 when compared with those of run SK1 were also found by Lalbeharry (2002). The WM1, KM2 and SJ2 scatter plots appear quite similar, that is, WAM4.5, as implemented here, can be used in an operational environment by CMC to produce wave forecasts for the Great Lakes. Fig. 6 is the same as Fig. 5 but for peak periods. Lake Erie is wind sea dominated with peak periods mostly below 8 s. All the model runs show more scatter of peak periods than wave heights when compared with buoy observations. There is a general tendency to underpredict the peak periods.

Fig. 7 presents the two-dimensional (2-d) spectra for model runs WM1, KM2, SJ2 and SK1 at buoy location 45132 valid 1500 UTC 13 November 2003 near the occurrence of buoy peak
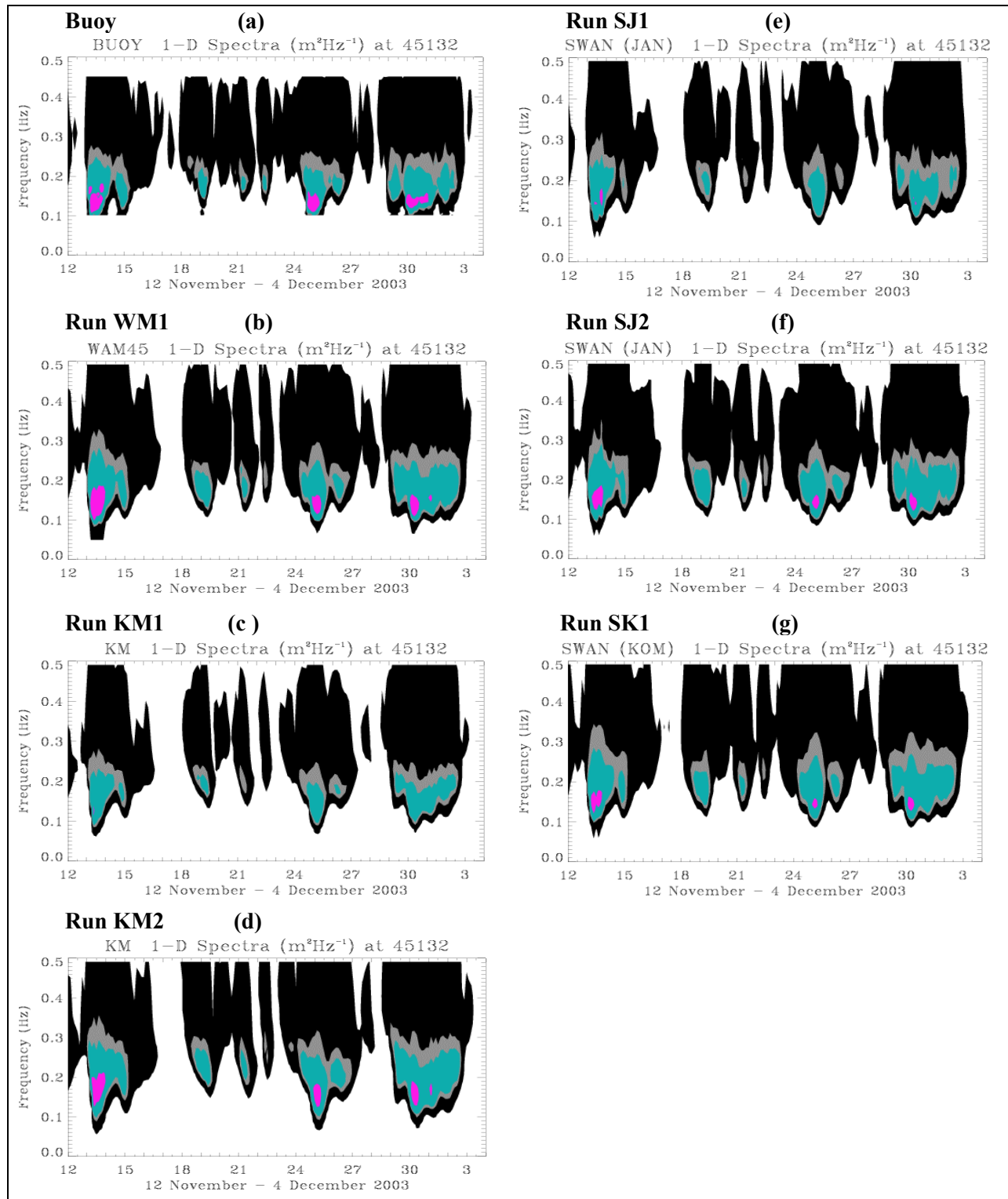
Fig. 2: Time series plots of the buoy and model one-dimensional spectra at 3-hourly intervals at the location of buoy 45132 for the period 12 November - 4 December 2003. The spectra shown are (a) buoy, (b) the WAM4.5 run WM1, (c) - (d) the K-model runs KM1 and KM2 defined in Table 2, and (e) - (g) the SWAN runs SJ1, SJ2 and SK1 defined in Table 1. The colored areas are energy density levels in m^2 Hz^{-1} , namely, black (0.025 - 0.5), gray (0.5 - 1.0), turquoise (1.0 - 10.0) and rose (10.0 - 20.0).
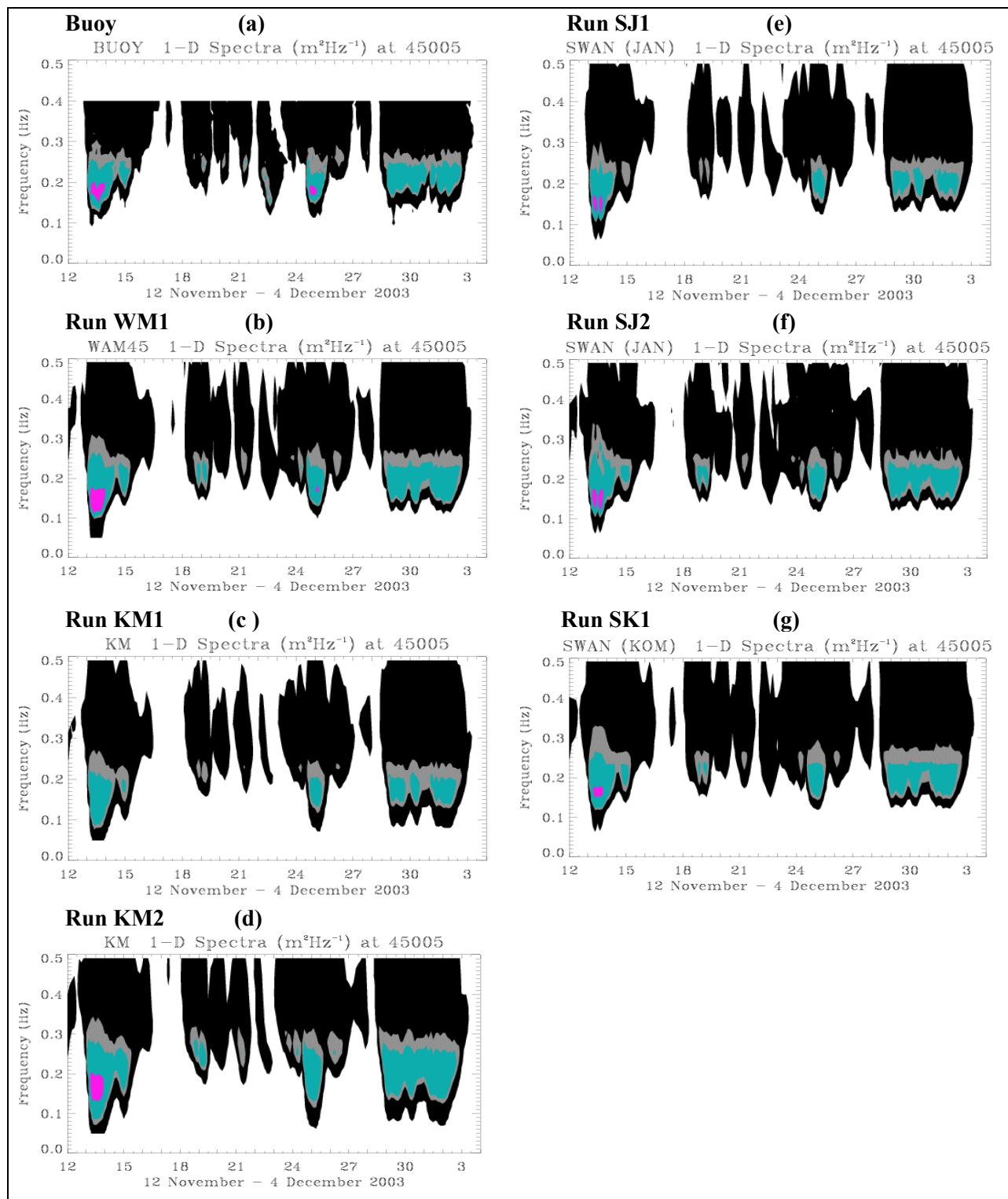
Buoy **(a)**

BUOY   1−D Spectra (m²Hz⁻¹) at 45005

Run WM1 **(b)**

WAM45   1−D Spectra (m²Hz⁻¹) at 45005

Run KM1 **(c)**

KM   1−D Spectra (m²Hz⁻¹) at 45005

Run KM2 **(d)**

KM   1−D Spectra (m²Hz⁻¹) at 45005

Run SJ1 **(e)**

SWAN (JAN)   1−D Spectra (m²Hz⁻¹) at 45005

Run SJ2 **(f)**

SWAN (JAN)   1−D Spectra (m²Hz⁻¹) at 45005

Run SK1 **(g)**

SWAN (KOM)   1−D Spectra (m²Hz⁻¹) at 45005

Fig. 3: Same as Fig. 2 but for buoy 45005.

Model runs WM1, KM2 and SJ2
(a)

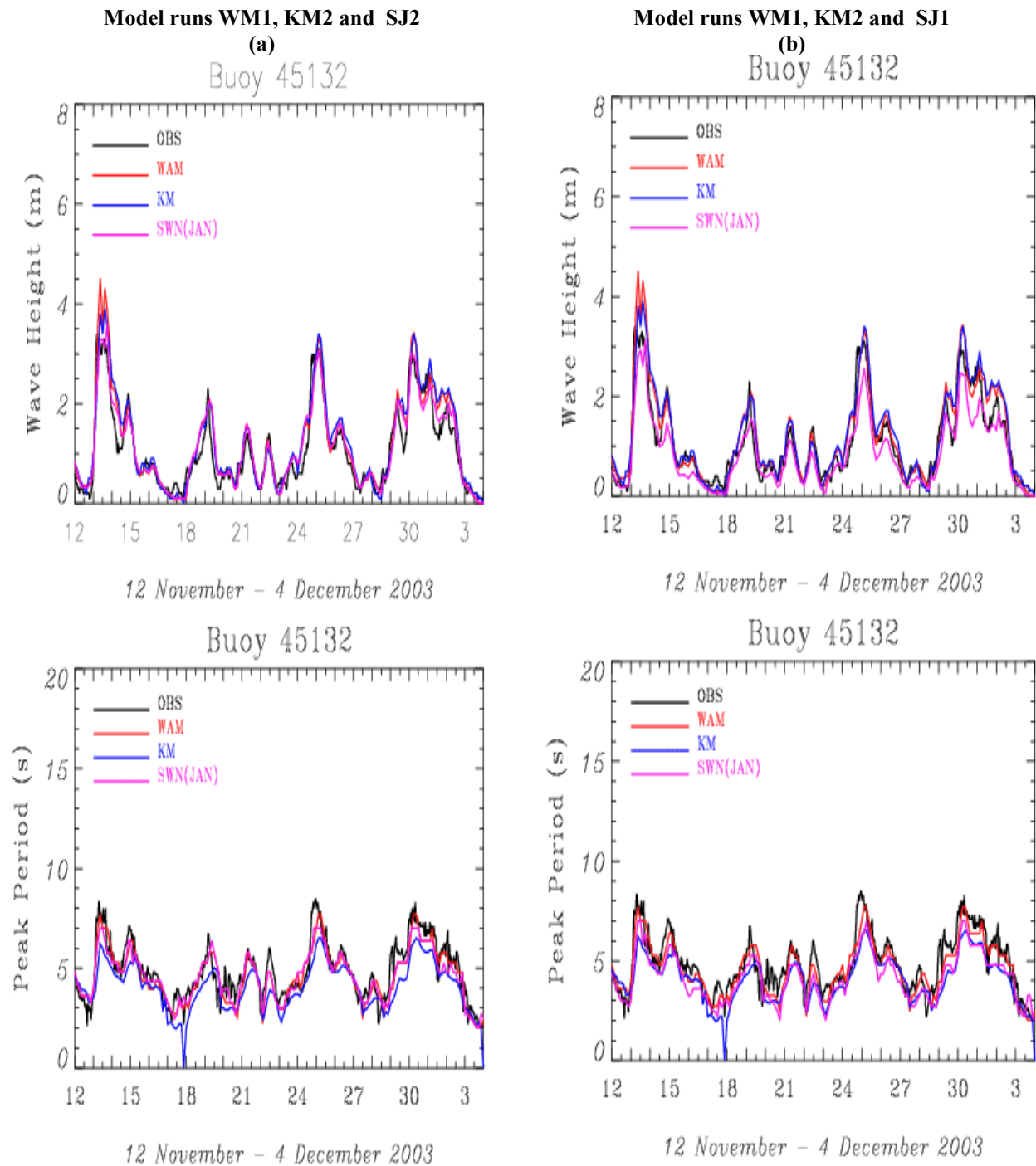**Model runs WM1, KM2 and SJ1**
(b)

Fig. 4: Time series of observed and model wave heights and peak periods at buoy location 45132 for the period 12 November - 4 December 2003. In the figure, observed values are denoted by black lines, the WAM4.5 run WM1 values by red lines, the K-model run KM2 values by blue lines and the SWAN values by rose lines for run SJ2 in (a) and for run SJ1 in (b). See Table 1 for the K-model and Table 2 for the SWAN run identifications. In the legend "JAN" indicates Janssen's formulation of WAM4.
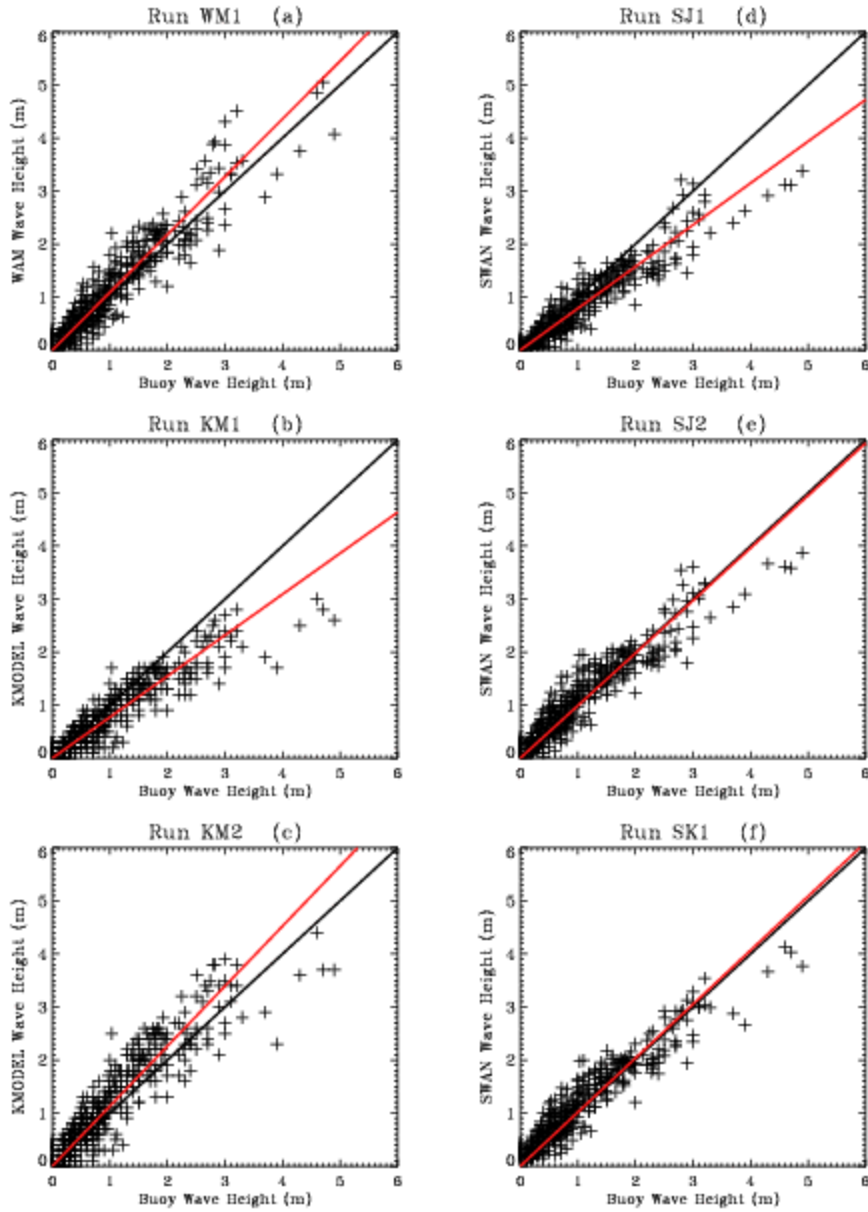
Fig. 5: Scatter plots of model versus observed wave heights based on observations at buoys 45005, 45132 and 45142 for the period 12 November - 4 December 2003. In the figure, WM1 denotes the WAM4.5 run, KM1 and KM2 the K-model runs defined in Table 2 and SJ1, SJ2 and SK1 the SWAN runs defined in Table 1. The black lines denote the perfect fit to model and observed values and the red lines the symmetric slope, s, as defined in Table 4. Model values are overpredicted for $s > 1.0$ and underpredicted for $s < 1.0$.
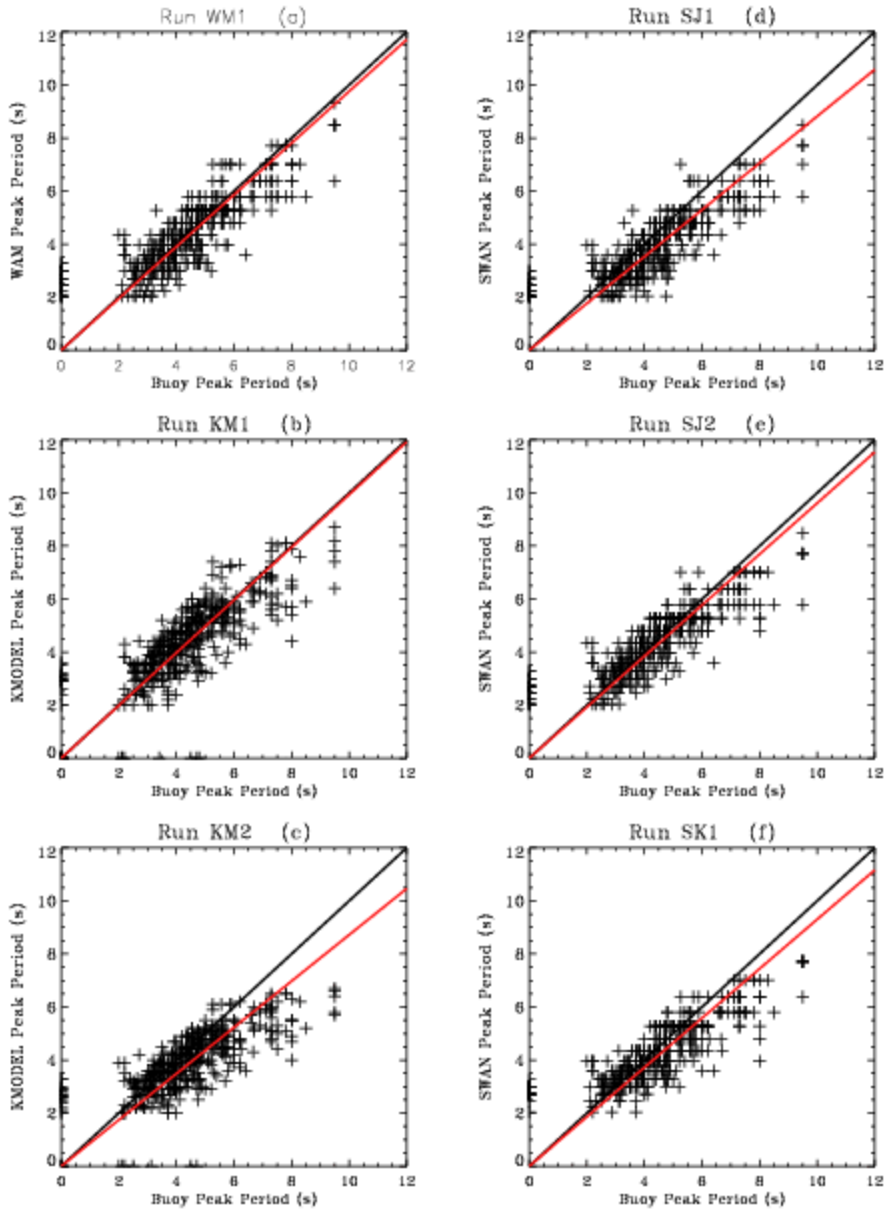
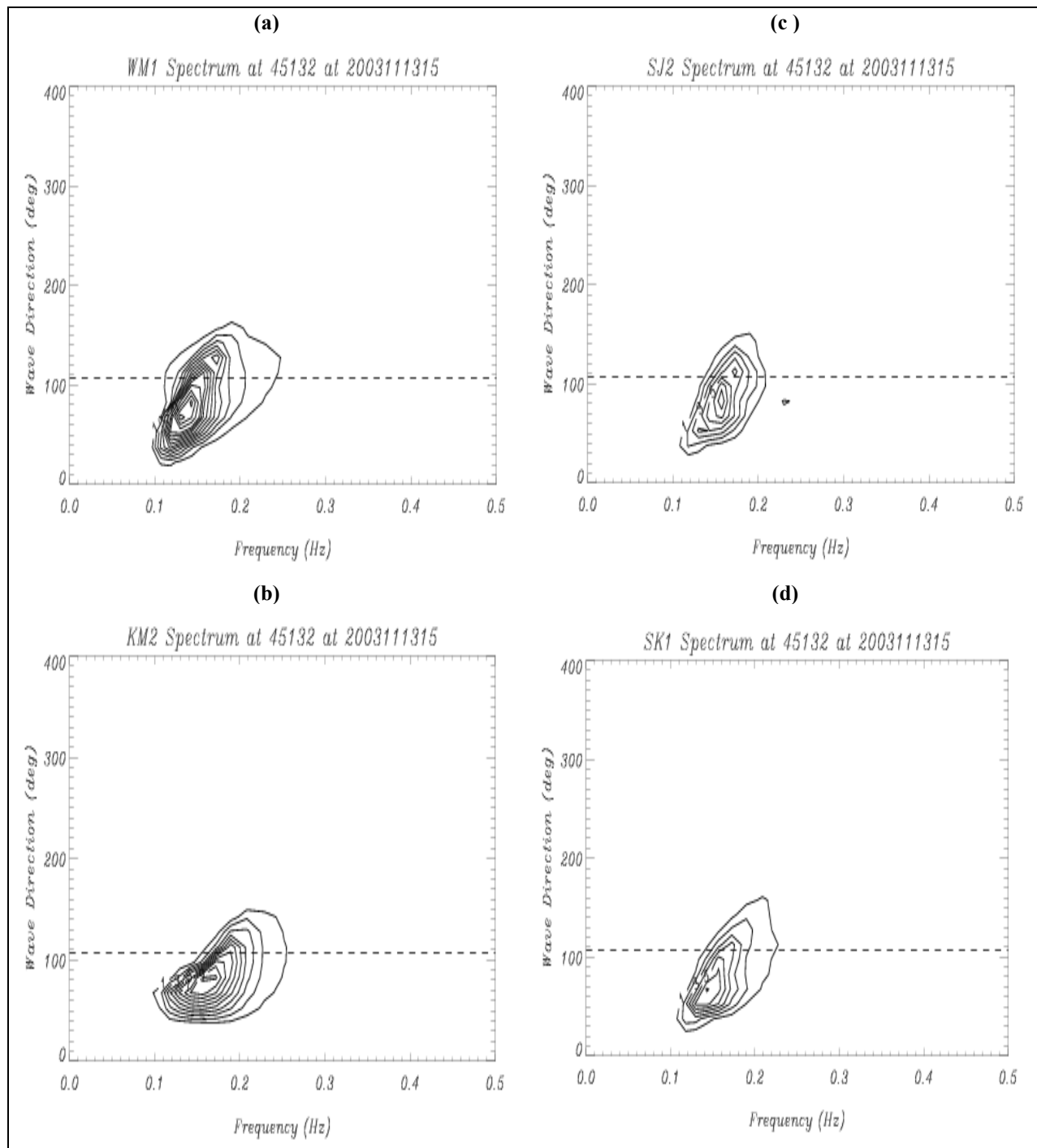Fig. 6: Same as Fig. 5 but for peak periods.

(a)

WM1 Spectrum at 45132 at 2003111315

(c)

SJ2 Spectrum at 45132 at 2003111315

(b)

KM2 Spectrum at 45132 at 2003111315

(d)

SK1 Spectrum at 45132 at 2003111315

Fig. 7. Model two-dimensional spectra in $m^2Hz^{-1}rad^{-1}$ valid 1500 UTC 13 November 2003. The dashed line is the direction to which the wind is blowing. Contours are spectral energy density in $m^2Hz^{-1}rad^{-1}$ and are given at intervals of 1 unit up to the first 10 units of energy density and at intervals of 2 units thereafter.

Table 4: Validation statistics for wave heights >= 0.1 m and peak periods >= 2.0 s for the period 12 November - 4 December 2003 for the different model runs. Here, **Bias = 1/n𝛴(Xᵢ - Yᵢ)** is the mean error, **stddev = [1/N𝛴(Xᵢ - Yᵢ - Bias)²]¹ᐟ²** the standard deviation of errors, **SI = stddev/(Buoy Mean)** the scatter index, **r = [1/N𝛴(Yᵢ - Y_{mean})(Xᵢ - X_{mean})]/σ_yσ_x** the linear correlation coefficient, **ac = 𝛴(Yᵢ - X_c)(X - X_c)/[𝛴(Yᵢ - X_c)²(X - X_c)²]¹ᐟ²** the anomaly correlation, **rv = 1 - 𝛴(Yᵢ - X_c)²(X - X_c)²** the reduction of variance and **s = [𝛴Yᵢ²/𝛴Xᵢ²]¹ᐟ²** the symmetric slope, where X_i and Y_i are, respectively, the ith observed and model values, X_c the climaltology of X, σ_y the standard deviation of Y, σ_x that of X and N the number of observations. WM1 denotes the WAM4.5 run, KM1 and KM2 the K-model runs defined in Table 2 and SJ1, SJ2 and SK1 the SWAN runs defined in Table 1.

	WAVE HEIGHT STATISTICS (m)					
	WAM	KMODEL	KMODEL	SWAN	SWAN	SWAN
Run ID	WM1	KM1	KM2	SJ1	SJ2	SK1
Buoy mean	1.043	1.043	1.043	1.043	1.043	1.043
Model mean	1.136	0.819	1.204	0.815	1.076	1.119
Bias	0.093	-0.224	0.161	-0.228	0.033	0.076
Stddev	0.319	0.360	0.376	0.310	0.291	0.277
SI	0.305	0.345	0.361	0.297	0.279	0.265
r	0.938	0.919	0.912	0.941	0.938	0.945
ac	0.927	0.887	0.890	0.910	0.934	0.933
rv	0.844	0.746	0.764	0.791	0.879	0.884
s	1.089	0.772	1.131	0.787	0.989	1.016
N (no. of obs.)	412	412	412	412	412	412

	PEAK PERIOD STATISTICS (s)					
	WAM	KMODEL	KMODEL	SWAN	SWAN	SWAN
Run ID	WM1	KM1	KM2	SJ1	SJ2	SK1
Buoy mean	4.591	4.591	4.591	4.591	4.591	4.591
Model mean	4.479	4.542	4.008	4.046	4.441	4.294
Bias	-0.112	-0.050	-0.583	-0.545	-0.150	-0.298
Stddev	0.778	0.974	0.973	0.794	0.773	0.810
SI	0.169	0.212	0.212	0.173	0.168	0.176
r	0.846	0.768	0.745	0.840	0.850	0.836
ac	0.834	0.754	0.704	0.803	0.839	0.826
rv	0.717	0.563	0.409	0.574	0.716	0.658
s	0.967	0.987	0.864	0.874	0.952	0.919
N (no. of obs.)	411	411	411	411	411	411

wave height shown in Fig. 4. The three models show quite similar 2-d spectral patterns with the individual model peak wave direction close to the wind direction. However, peak intensities vary from one model to the other and reflect the overprediction of wave heights in the WM1 and KM2 runs. The wave heights in the SJ2 and SK1 runs are in closer agreement with the observed wave height and this is also reflected in their corresponding 2-d spectra. The fact that each model shows generally the same frequency of the peak 2-d energy suggests that the absence of the source term S_{nl4} in the K-model has

minimal impact as observed also in the 1-d spectra in Figs. 2 and 3.

The validation statistics for wave heights >= 0.1 m and peak periods >= 2.0 s obtained from the various model runs against buoy measurements are presented in Table 4. They quantify the model performances discussed in the preceding paragraphs. In the computations of the anomaly correlation, ac, and the reduction of variance, rv, the buoy mean is used as the climatology. ac and rv are skill scores since they provide a measure of how much more skill the model hindcast has over the unskilled estimate

based on climatology. The hindcast is considered to be useful if the ac exceeds the threshold value of 0.6 or 60% (Janssen, 1997). For rv > 0.0 the hindcast is better than climatology. In the wave modelling community the definition of scatter index (SI) involving the standard deviation of errors instead of the rmse is now more commonly used.

Examination of the wave height statistics indicate that the models show skill in the sense that the ac > 60% and the rv is all positive. The K-model runs KM1 and KM2 shows marginal differences except for the bias. The magnitude of the KM1 bias is about 1.4 times the magnitude of the KM2 bias. This is due to mainly the larger underprediction at higher wave heights. In the case of the SWAN runs SJ2 outperforms SJ1 and is in close agreement with SK1. The WM1 statistics agree better with the SJ2 statistics rather than with those of SJ1. The results are encouraging since models with WAM4 implementation should produce statistics in close agreement.

For the peak period statistics the three models are consistent in that all have negative biases and small differences in SIs. The SI values range from 0.17 to 0.21. An SI value of 0.15 is considered to be quite good. The models show skill although to a lesser extent than for wave heights. The peak period is similarly defined in each model. Although the peak energy may vary from one model to the other, the period of the peak energy may not vary significantly. This can be seen in Fig. 2 and may account for the close agreement among the peak period statistics of the three models.

4. SUMMARY AND CONCLUSIONS

In this study three third generation state-of-the-art ocean wave models, namely, the WAM4.5, K-model and SWAN are used in a hindcast mode to generate waves in Lake Erie dominated by locally generated wind seas during the period 12 November - 4 December 2003. The models described in section 2 are applied in shallow water mode with depth refraction only and the results obtained by each of the models are validated against observations primarily at 3 buoy locations shown in Fig. 1. In the K-model two different parameter sets given in Table 2 are used. It is shown that the results of the K-model depend sensitively on the choice of the appropriate parameter set for the spatial resolution of the model grid. The parameter set corresponding to run KM2 is better able to simulate the peak wave heights of the main wave episodes shown in Figs. 1 and 2. The modified version of the SWAN implementation of WAM4 produces wave heights that are more accurate than

those of the unmodified version and are in closer agreement with the results using the WAM3 option of SWAN and with those of WAM4.5 The WAM4.5, the K-model run KM2 and the SWAN runs SJ2 and SK1 slightly overpredict the wave heights and underpredict the peak periods. The statistical analysis shows that the three models provide comparable results although the K-model neglects the wave-wave nonlinear interaction source term and uses a nonlinear dissipation source term.

5. REFERENCES

Booij, N., R. C. Ris and L. H. Holthuijsen, 1999: A third generation wave model for coastal regions 1. Model description and validation. J. Geophy. Res., 104, C4, 7649-7666.

Cavaleri, L. and P. Malanotte-Rizzoli, 1981: Wind wave prediction in shallow water: Theory and applications. J. Geophys. Res., 86, 10961-10973.

Hasselmann, K., T. P. Barnett, K. Bouws, H. Carlson, D. E. Cartwright, K. Enke, J. I. Ewing, H. Gienapp, D. E. Hasselmann, P. Kruseman, A. Meerburg, P. Muller, K. Richter, D. J. Olbers, W. Sell and H. Walden, 1973: Measurements of wind-wave growth and swell decay during the Joint North Sea Wave Project (JONSWAP), Dtsch. Hydrogr. Z. Suppl., 12, A8, 95p.

Hasselmann, S., K. Hasselmann, J. H. Allender and T. P. Barnett, 1985: Computations and parameterizations of the nonlinear energy transfer in a gravity-wave spectrum. Part II: Parameterizations of the nonlinear transfer for application in wave models. J. Phys. Oceanogr., 19, 745-754.

Hersbach, H. and P. A .E. M. Janssen, 1999: Improvement of the short-term behaviour in the wave ocean model (WAM). J. Atmos. Oceanic Techn., 16, 884-892.

Janssen, P. A. E. M., B. Hansen, and J. R. Bidlot, 1997: Verification of the ECMWF wave forecasting system against buoy and altimeter data. Wea. Forecasting, 12, 763-784.

———, 1989: Wave-induced stress and the drag of air flow over sea waves J. Phys. Oceanogr., 19, 745-754.

——— , 1991: Quasi-linear theory of wind-wave generation applied to wave forecasting. J. Phys. Oceanogr., 21, 1631-1642.

Komen, G. J., L. Cavaleri, M. Donelan, K. Hasselmann, S. Hasselmann, and P. A .E. M. Janssen, 1994: Dynamics and Modelling of Ocean Waves, Cambridge University Press, Cambridge, 532p.

———— , S. Hasselmann and K. Hasselmann, 1984: On the existence of a fully developed windsea spectrum. J. Phys. Oceanogr., 14, 1271-1285.

Lalbeharry, Roop, 2002: Comparison of the performances of three state-of-the-art ocean wave models in extreme storm cases. Proc., 7th Int. Workshop on Wave Hindcasting and Forecasting, Banff, Alberta, October 21-25, 2002. Published by Environment Canada

Ris, R. C., L. H. Holthuijsen and N. Booij, 1999: A third generation wave model for coastal regions 2. Verification. J. Geophy. Res., 104, C4, 7667-7681.

————, 1997: Spectral modelling of wind waves in coastal areas. PhD Thesis, Delft University of Technology, Delft, Netherlands.

Schneggenburger, C., 1998: Spectral wave modelling with nonlinear dissipation. PhD thesis, University of Hamburg, GKSS External Report, 98/E/42.

————, H. Guenther and Wolfgang Rosenthal, 2000: Spectral wave modelling with non-linear dissipation: validation and applications in a coastal tidal environment. Coastal Engineering, 41, 201,235.

SWAN, 2004: User Manual SWAN Cycle III version 40.31, February 5, 2004.   Delft University of Technology, Department of Civil Engineering, the Netherlands.

Tolman, H. J., 1992: Effects of numerics on the physics in a third generation wind-wave model. J. Phys. Oceanogr., 22, 1095-1111.

WAMDI Group, 1988: The WAM model - A third generation ocean wave prediction model. J. Phys. Oceanogr., 18, 1775-1810.